J. Sustain. Metall.
DOI 10.1007/s40831-016-0098-9

THEMATIC SECTION: GREEN RARE EARTH ELEMENTS–INNOVATIONS IN ORE PROCESSING, HYDROMETALLURGY, AND ELECTROLYSIS

Precipitation Trends of Scandium in Synthetic Red Mud Solutions with Different Precipitation Agents

Bengi Yagmurlu[1,2] · **Carsten Dittrich**[1] · **Bernd Friedrich**[2]

Abstract This research presents an alternative method for scandium (Sc) recovery from impure bauxite residue solutions containing Fe(III), Al, Ca, Nd, and Y through the use of hydroxide and phosphate precipitation. Among hydroxide donors, ammonia solution removed the most Fe(III) from solution, while co-precipitation of other elements in the synthetic pregnant leach solution remained negligible. When using dibasic phosphate as the precipitant, in the pH range of 1.5–2.5, both Sc and Fe were removed rapidly, while co-precipitation of other ions remained low. Experimental results were used to propose the preliminary design of a three-stage precipitation process capable of producing a scandium product from highly impure process solutions.

Keywords Scandium · Bauxite residue · Red mud · Precipitation · Recovery

Introduction

Scandium (Sc) is an extremely expensive element for industrial usage at the moment. However, despite its price, the demand of Sc is increasing worldwide owing to the recent developments of a wide range of promising applications. The Al–Sc alloys, which mainly target aeronautical and transportation industries, sporting equipment, and military demand, have superior properties compared to its counterparts: high thermal resistance, light weight, and high strength as well as can be proposed as a solution to problems occurring during welding operations in aluminum [1–3]. In addition, the extreme oxygen-ion conductivity of scandia-stabilized zirconia makes it a suitable material for use in solid-oxide fuel cells [4, 5].

Due to very limited and rare direct sources of Sc ores, it must be extracted as a by-product which leads to complex metallurgical processes combined with high production and purification expenses. A lot of effort has been put to produce Sc as a by-product from uranium, tungsten, titanium, and nickel laterite ores using hydrometallurgical processes especially with ion-exchange and solvent extraction or the combination of both these processes [6–9]. Bauxite residue (i.e., red mud) is the by-product and the waste obtained from processing bauxite via Bayer process and is currently stockpiled in huge amounts all over the world. The estimated amount of red mud stocks is around four billion tonnes and it is continually growing [10]. The cost of transporting and depositing large amounts of bauxite residue affects both the production costs of aluminum and alumina and has a large potential for negative environmental impact, if not handled appropriately. Conversely, red mud can contain significant amounts of valuable elements, Ti, Sc, Y, Nd, Ce, and has the potential to be a precious resource.

As a result of the low concentration of Sc in bauxite residue leachates, previous studies regarding Sc recovery from bauxite residue were mainly focused on solvent extraction and ion-exchange processes [11–15]. Previous works considered bauxite residues obtained from different parts of the world, showing that nearly complete Sc

The contributing editor for this article was Yiannis Pontikes.

✉ Bengi Yagmurlu
bengi@meab-mx.com

[1] MEAB Chemie Technik GmbH, Dennewartstr. 25, 52068 Aachen, Germany

[2] IME Institute of Process Metallurgy and Metal Recycling, RWTH Aachen, Intzestr. 3, 52056 Aachen, Germany

Published online: 03 November 2016

recovery was achieved by the proposed processes. Unfortunately, due to high concentrations of Fe, Al, and Ti, co-extraction became a problem for these hydrometallurgical operations, and intensive purification was therefore required to produce a high-quality product.

This paper investigates a different approach for Sc recovery from bauxite residue: precipitating Sc with different precipitation agents and co-precipitating the major constituent elements of the synthetic red mud leachates used in the work.

Experimental Procedure

A red mud sample was obtained from Aluminium of Greece, subject to lithium borate fusion, and analyzed using ICP-MS/AAS, as shown in Table 1 (Vassiliadou V., internal communications, 2015).

EU H2020 ETN Red Mud is a collaborative project between industry and research institutes and mainly focuses on complete valorization of the bauxite residue. As a member of this project, this study considers the expected pregnant leach solutions (PLS) obtained by sulphuric acid leaching after recovering Fe by pyrometallurgical methods, Al by combining pyrometallurgical and hydrometallurgical processes, and Ti by liquid extraction procedures in accordance with the recent developments by linked studies within the project. Hence, the synthetic solution mentioned in this study is the predictive of the speciation of real PLS in cooperation with the linked studies. The synthetic bauxite residue PLS was designed by considering the major impurity elements (e.g., Fe, Al, and Ca), as well as the minor ones, Nd and Y. These REEs was preferred as the representative elements of light and heavy group, since the sub-groups of REEs distinguishes similar chemical properties.

Synthetic solutions were prepared by adding the required amount of $Fe_2(SO_4)_3{\cdot}9H_2O$, $Al_2(SO_4)_3{\cdot}18H_2O$, $Sc_2(SO_4)_3{\cdot}5H_2O$, $NdCl_3{\cdot}6H_2O$, and $YCl_3{\cdot}6H_2O$. Chloride salts were first precipitated as hydroxides and converted into sulfate before addition to avoid unwanted chlorine ions which can result in unwanted complex formation. Considering the conversion of Fe(II) to Fe(III) in open system, to form a synthetic solution similar to the real one, only Fe(III) was chosen to be used in the solution. All precipitation solutions were prepared from reagent-grade salts. Concentrations of the precipitation agents were 12.5 wt% for $CaCO_3$ (limestone) slurry, 1 mol/L for NaOH, NH_3(aq), and KOH, 0.1 mol/L for hexamethylenetetramine (HMTA), and 1 mol/L for K_2HPO_4, $(NH_4)_2HPO_4$, and Na_2HPO_4.

The concentration of the synthetic PLS is presented in Table 2. To investigate the precipitation behaviors, synthetic solution was prepared by using the reagent-grade salts of the existing ions, and sulphuric acid was added to aqueous solution in order to maintain pH between 1.2 and 1.4. In all the precipitation trials, the same PLS composition was used to compare the effects of different experimental conditions and precipitants used.

The precipitation agents mentioned were carefully dripped using precision burette into 50 mL of the synthetic PLS while monitoring the pH and temperature. All experiments presented in this study were performed at room temperature. For hydroxide precipitation, agents were added until the target pH was attained under mild agitation to reach homogeneity in the solution and to prevent local pH differences.

For hexamethylenetetramine, precipitant solution (0.1 mol/L) with varying volumes, 50, 75, 100, and 125 mL, were dripped into 100 mL of solution at a rate of 5 mL/min to ensure the required amount of ammonia was released from the reagent. The pH and the temperature were carefully monitored during addition.

Precipitation solution of dibasic phosphates (1 mol/L) was added to the 50 mL synthetic PLS starting with 0.5 mmol, and in each case the amount added was doubled until pH > 5 was reached. Dibasic phosphates were chosen to observe the behavior of precipitation at different pH ranges.

The resulted suspension for each case is then stabilized and homogenized at a given pH and temperature for 2 h and subsequently filtered through fine filter paper via

Table 1 Chemical composition of the red mud (Vassiliadou V., internal communications, 2015)

Major compounds	%	Minor compounds	%
Fe_2O_3	42.34	La_2O_3	0.09
Al_2O_3	16.25	CeO_2	0.06
CaO	11.64	Sc_2O_3	0.02
SiO_2	6.97	Nd_2O_3	0.01
TiO_2	4.27	Y_2O_3	0.01
Na_2O	3.83	Others	1.85
LOI	12.66		

Table 2 Composition of the synthetic PLS obtained from red mud after the recovery of Fe, Al, and Ti

	Concentration(mg/L)
Al	450
Fe(III)	400
Ca	250
Sc	100
Y	100
Nd	100

suction filtration. The separated solid residue was washed with distilled water and dried at 110 °C for 24 h. Both filtered solutions and the solid residues were assayed.

The concentrations of the constituent ions of Fe, Al, Sc, Y, and Nd were determined by microwave plasma optical emission spectroscopy (Agilent MP-AES 4100). Each sample was prepared by adding 100 µL of caesium ionization buffer and 500 µL of ultrapure concentrated HNO_3 to 10 mL of sample solution. Quantitative analyses were performed at 371.993, 396.152, 361.383, 371.029, and 430.358 nm spectral emission lines for Fe, Al, Sc, Y, and Nd, respectively.

The measurements for pH were performed using WTW ProfiLine pH 197 series pH-meter with Sentix 81 precision electrode. The pH meter was calibrated with standard technical buffering solutions at pH 2.00, 4.01, and 7.00 to achieve maximum sensitivity in pH measurements.

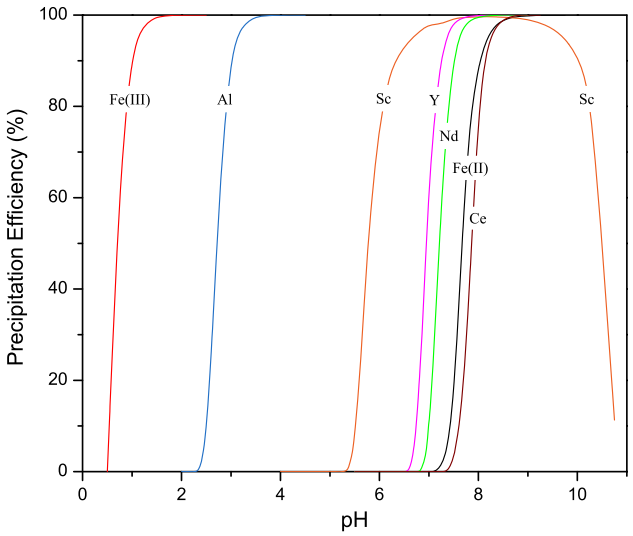

Fig. 1 Visual MINTEQ simulation for hydroxide precipitation from red mud leachate

Results and Discussion

Simulation of the Solution System

Visual MINTEQ^{TM} is a software capable of simulating equilibrium states of the species while taking into consideration the thermodynamic parameters, and can be also used to calculate the equilibrium composition of aqueous solutions. The precipitation mechanism of the red mud leachate was simulated by the addition of required amount of OH^- ions to the system to reach the target pH value. Figure 1 clearly indicates the dependencies of pH and the precipitation ranges of the constituent ions in the solution. According to this figure, precipitation order is resolved as

$$Fe^{3+} > Al^{3+} > Sc^{3+} > Y^{3+} > Nd^{3+} > Fe^{2+} > Ce^{3+}$$

Although Sc precipitation completed at pH 8, after reaching this point Sc starts to dissolve again in the system according to the simulated solution system as a consequence of stabilization of $Sc(OH)_6^{3-}$ complex which is soluble in highly alkaline environment [16].

According to the simulation results of the solution system, Fe(III) and Al can be completely separated from the other constituents in the solution easily by hydroxide precipitation; however, the formation of intermediate complexes and interactions of ions with each other in the multicomponent system during precipitation was ignored by the software. Since the major problem of the scandium recovery by precipitation from multicomponent solution is co-precipitation with ions presented in the system, especially with iron, experimental investigation of the system is necessary.

Hydroxide Precipitation

In order to observe the precipitation behavior of Sc with both conventional and unconventional precipitation agents, solution containing only 0.5 g/L Sc was tested. Figure 2 demonstrates the experimental results of precipitation of $Sc(OH)_3$ with limestone, NaOH, NH_3(aq), and HMTA. The conventional hydroxide precipitation agents, limestone, NaOH, and NH_3(aq), showed similar behavior in the absence of other constituent ions. The precipitation begins from the addition of the agents, has plateaus between pH 2 and 5, and then is followed with the rise of the precipitation rate until the completion of the reaction.

On the other hand, HMTA, which undergoes a slow hydrolysis reaction that results in the release of formaldehyde and ammonia in low pH or elevated temperatures, exhibits a totally different behavior when compared to the rest of the solutions [17, 18]. In this case, immediate pH change was not detected upon addition, due to slow decomposition of the precipitation agent. However, as a result of ammonia discharge in acidic environment, precipitation started with the addition of the agent to the system.

Addition of limestone, NaOH, NH_3(aq), and KOH to synthetic multi-element red mud solution was investigated as well, and the precipitation trends of the ions in the system is shown in Fig. 3. Since the release of formaldehyde gas upon adding HMTA into the acidic system is toxic, this precipitation agent was not used in these comparisons.

The first aim is to remove Fe(III) from the system with minimal amount of co-precipitation of the other ions in the solution. Addition of limestone slurry to the system

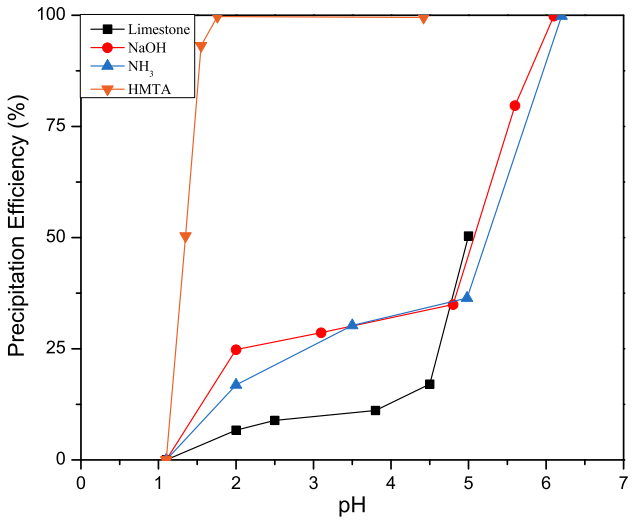

Fig. 2 Hydroxide precipitation with limestone, NaOH, NH_3, and HMTA of solution containing only 0.5 g/L Sc

initially triggered the Fe(III) precipitation around pH 2.8 which then finalizes the precipitation at pH 3.5. During complete Fe(III) precipitation, all other elements were co-precipitated around 15–20 %. Similar precipitation behavior was also seen in the case of NaOH and KOH addition where Fe(III) precipitation was observed to occur between pH 2.5 and 3.5, and co-precipitation of the other ions was in the range between 15 and 30 % for both precipitants. The precipitation of these elements was in the order Fe(III) > Al ≈ Sc > Y = Nd.

In the case of NH_3(aq) addition, Fe(III) precipitation started at pH 3.1 and terminated at approximately pH 3.8. The minimum co-precipitation values were obtained with the addition of ammonia solution to the system. When Fe(III) was almost completely eliminated from the system, Sc and REE losses were between 4 and 10 %. This indicates that ammonia addition is superior, compared to other hydroxide donors with regard to the co-precipitation of valuable and recoverable ions in the system. A possible reason for low Sc co-precipitation as Fe(III) is almost completely precipitated unlike other precipitants is because of the occurrence of scandium hexammine complex upon addition of ammonia to the system. This can inhibit the interaction between Fe and Sc and prevent co-precipitation in the system [16, 19, 20].

Analogous to solvent extraction parameters, selectivity coefficients (S) can also be used as a suitable tool to compare the selectivity of the different precipitation agents. Selectivity of the element A over B can be calculated using the following equation:

$$D_A = \frac{C_{prec}}{C_{aq}} \quad \text{and} \quad S_{A/B} = \frac{D_A}{D_B}, \tag{1}$$

where D_A or D_B is the distribution coefficient of the mentioned element; C_{prec} is the concentration of the element in the precipitate; C_{aq} is the concentration of the element in the aqueous solution after precipitation; and $S_{A/B}$ is the selectivity coefficient which indicates the selectivity of A over B.

Tables 3 and 4 shows the critical pH values for Fe(III) removal by comparing all the precipitation agents according to precipitation efficiency and indicates the selectivity coefficients of Fe(III) over Sc.

As clearly seen from Tables 3 and 4, in all cases, ammonia solution showed superior selectivity when compared to the other precipitation solutions. The most efficient precipitation agent for partial and nearly complete Fe(III) removal while keeping Sc and the other recoverable precious ions in the solution is the ammonia solution within the pH range of 3.3–3.6.

Phosphate Precipitation

This section of the study investigates the precipitation of Sc and REEs by the addition of 1 mol/L dibasic phosphate solutions. Previous studies showed that Y^{3+} and REE ions indicated strong affinity towards PO_4^{3-}, compared to SO_4^{2-} upon the addition of phosphate salts to sulfate solution of Y and REEs [21–24]. Due to the behavioral similarities between Sc and REEs, similar precipitation behavior can be triggered by the addition of dibasic salts.

Dibasic salts, K_2HPO_4, $(NH_4)_2HPO_4$, and Na_2HPO_4, were tested for Sc precipitation:

$$\mathrm{REE}(\mathrm{SO_4})_n^{3-2n}(\mathrm{aq}) + \mathrm{PO_4^{3-}}(\mathrm{aq}) \rightarrow \mathrm{REEPO_{4(s)}} + n\mathrm{SO_4^{2-}}(\mathrm{aq}) \tag{2}$$

These specific dibasic phosphates were chosen to observe the effect of pH on precipitation efficiency and precipitated products without addition of basic solutions. Upon dissolution in aqueous solutions, these dibasic phosphates decompose into its base (KOH, NH_3, and NaOH in this specific case) and the phosphate ion, so the favored complexes formed with different reactions in various pH values can also be observed.

The precipitation behavior of Sc in a pure solution with dibasic phosphate salts is shown in Fig. 4 with respect to change in pH values. Immediate precipitation was observed after the addition of these precipitation solutions. For all of the cases, precipitation was finalized between pH 2 and 3 and all of the precipitation agents showed similar behavior in the absence of another impurity ion.

When impurity ions were introduced into the system, the precipitation agents again showed similar behaviors as observed in the pure solution. However, the efficiencies of the reactions are distinctive for each case. Figure 5 shows

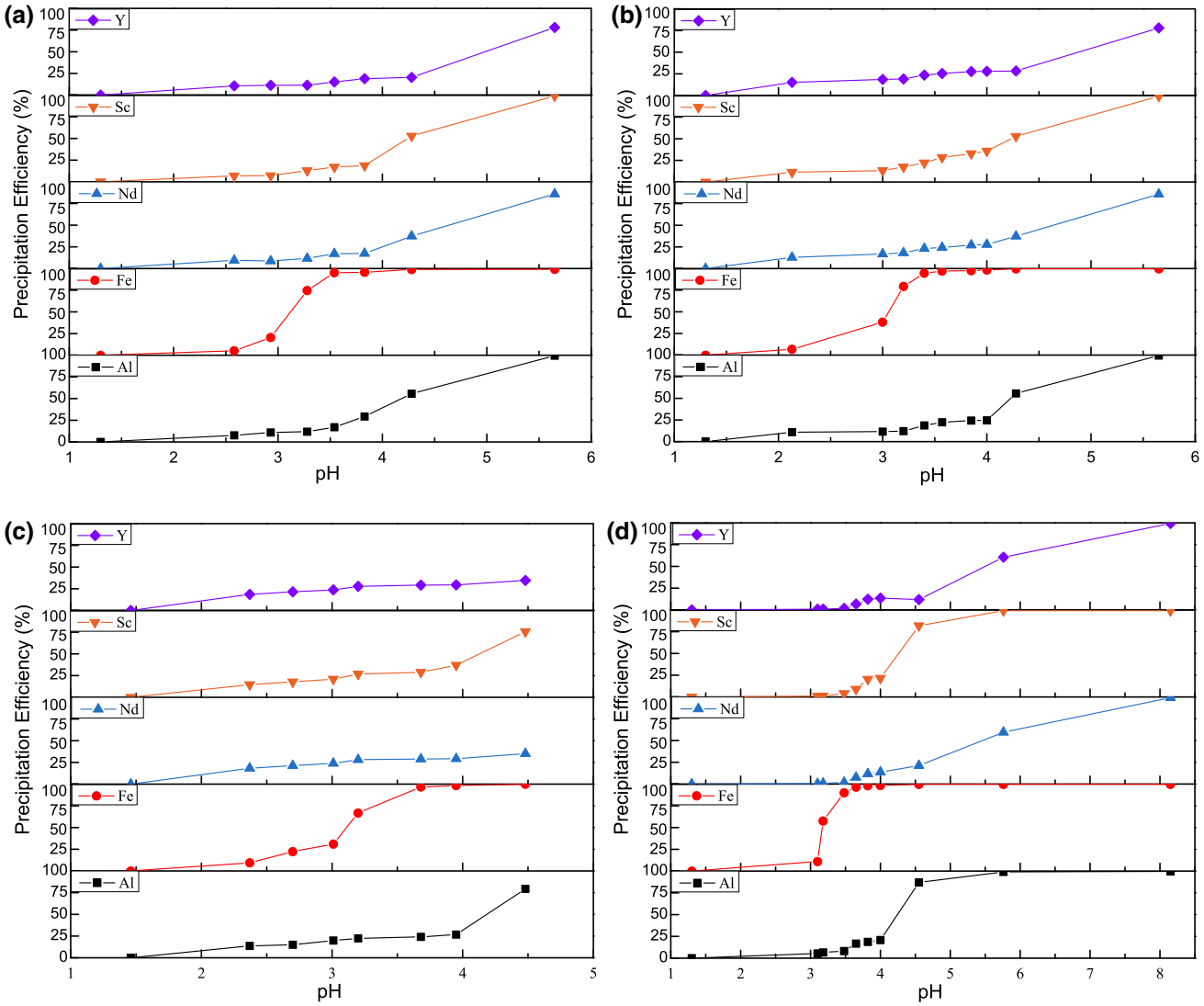

Fig. 3 Hydroxide precipitation of synthetic red mud leachate solution by **a** limestone, **b** NaOH, **c** KOH, and **d** NH_3(aq)

Table 3 Critical pH values for 70 % Fe(III) removal from the system by hydroxide precipitation and precipitation % of the constituent ions with selectivity of Fe over Sc

Precipitation agent	pH	Fe (%)	Sc (%)	Al (%)	Y (%)	Nd (%)	$S_{Fe/Sc}$
Limestone	3.28	72.7	12.9	11.8	11.4	12.1	18
NaOH	3.16	71.3	16.4	11.9	19.0	17.7	13
KOH	3.20	69.7	26.7	22.4	27.7	28.1	6
NH_3(aq)	3.35	73.5	1.6	7.4	1.4	1.3	170

the precipitation trends of the individual ions present in the system after the addition of dibasic phosphate precipitation solution. Since protons were released via $H_xPO_4^{x-3}$ ($1 \leq x \leq 3$) during precipitation of the constituents with a pH change, it is postulated that there has been a change in reaction mechanism. For all cases, the precipitation was observed to be in the following order:

$$Sc = Fe(III) > Y = Nd > Al$$

Addition of K_2HPO_4 solution into the synthetic red mud leachate resulted in immediate reaction of both Sc and Fe(III), while the co-precipitation of the other impurities remained at low levels (Fig. 5a). Addition of 0.2 mmol of precipitation solution resulted in the precipitation of 73 % of Sc in the solution, while 66 % Fe, 7 % Al, 16 % Nd, and 17 % Y were co-precipitated at pH 1.35. Further additions of the precipitant increase the pH and alter the stability of

Table 4 Critical pH values for >90 % Fe(III) removal from the system by hydroxide precipitation and precipitation % of the constituent ions with selectivity of Fe over Sc

Precipitation agent	pH	Fe (%)	Sc (%)	Al (%)	Y (%)	Nd (%)	$S_{Fe/Sc}$
Limestone	3.54	95.1	17.0	14.8	15.1	17.1	95
Limestone	3.83	95.6	18.7	15.8	18.9	17.4	94
NaOH	3.40	94.6	22.1	18.7	23.6	23.1	62
NaOH	3.57	97.1	28.4	22.3	25.4	24.3	84
KOH	3.68	96.7	28.9	24.1	29.3	28.9	72
NH_3(aq)	3.48	92.1	4.0	8.4	1.9	1.9	280
NH_3(aq)	3.65	96.6	8.9	16.7	6.7	7.6	291
NH_3(aq)	3.82	98.1	20.4	18.7	12.3	11.8	201

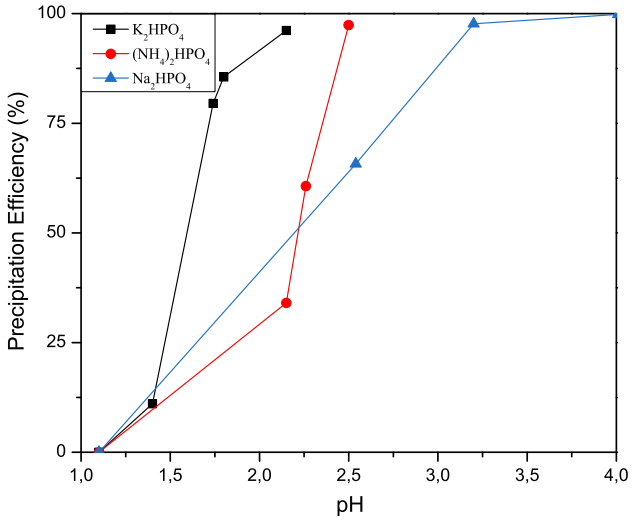

Fig. 4 Phosphate precipitation with K_2HPO_4, $(NH_4)_2HPO_4$, and Na_2HPO_4 of solution containing only 0.5 g/L Sc

the phosphate ion. When Sc is completely precipitated, 94 % of Fe, 34 % of Al, 51 % of Y, and 48 % of Nd were also co-precipitated.

In accordance with Fig. 5b, although $(NH_4)_2HPO_4$ solution showed analogous precipitation behavior with the K_2HPO_4 solution, rather than an instant reaction, it was observed that the reaction rate was lower than the others, but the co-precipitation percentages of the impurity ions were limited. 86 % of the Sc was recovered from the leachate, whereas 80 % Fe, 25 % Al, 18 % Y, and Nd were co-precipitated with Sc at pH 1.9. Once Sc was almost completely recovered from the solution, the precipitation efficiencies of Fe, Al, Y, and Nd were observed as 89, 37, 48, and 46 %, respectively. Furthermore, decomposition of $(NH_4)_2HPO_4$ into NH_3(aq) and its phosphate in aqueous solutions can be followed by the formation of hexammine complexes and the change in precipitation behavior than the other phosphates used.

Figure 5c shows the precipitation behavior of the synthetic red mud leachate upon the addition of Na_2HPO_4 solution. The precipitation behavior was very similar which was also detected in the case of K_2HPO_4 precipitation. As the precipitant was added to the solution system, precipitates immediately formed. 74 % Fe, 20 % Al, 32 % Y, and 29 % Nd were precipitated, whereas Sc had 79 % precipitation efficiency at pH 1.8. 92 % of Fe, 38 % of Al, 51 % of Y, and 49 % of Nd in the solution were precipitated from the system when almost complete Sc recovery was fulfilled.

Critical recovery percentages and the related pH values considering maximum Sc recovery with the lowest co-precipitation percentages of the ions in the solution are given in Table 5.

When the dibasic phosphate solutions were compared, the best pH range for low co-precipitation was established to be between 1.5 and 2.5. The precipitation efficiencies for all species in the system are observed to be higher once pH reaches greater values, owing to the additional complexes forming in the system, which is the main cause for this amplified yield. For instance, aside from $FePO_4$, precipitation of $Fe(OH)_3$ was also favored at higher pH values compared to the previously mentioned pH interval. The formation of hydroxide species at higher pH values also adversely affects the selectivity for Sc and Fe precipitation. In addition, in the pH range used, the phosphate complex has a higher thermodynamic stability than the double sulfate complex; thus, the final precipitates contained no double sulfates.

In terms of selectivity for Sc over the impurities in the solution, K_2HPO_4 was more selective for Sc compared to Na_2HPO_4 as shown in Table 6. On the other hand, $(NH_4)_2HPO_4$ displayed superior performance compared to other precipitation agents, for both partial and the complete Sc recovery from the solution. It has the highest Sc recovery percentages, in addition to lowest co-precipitation percentages among the dibasic phosphate salts.

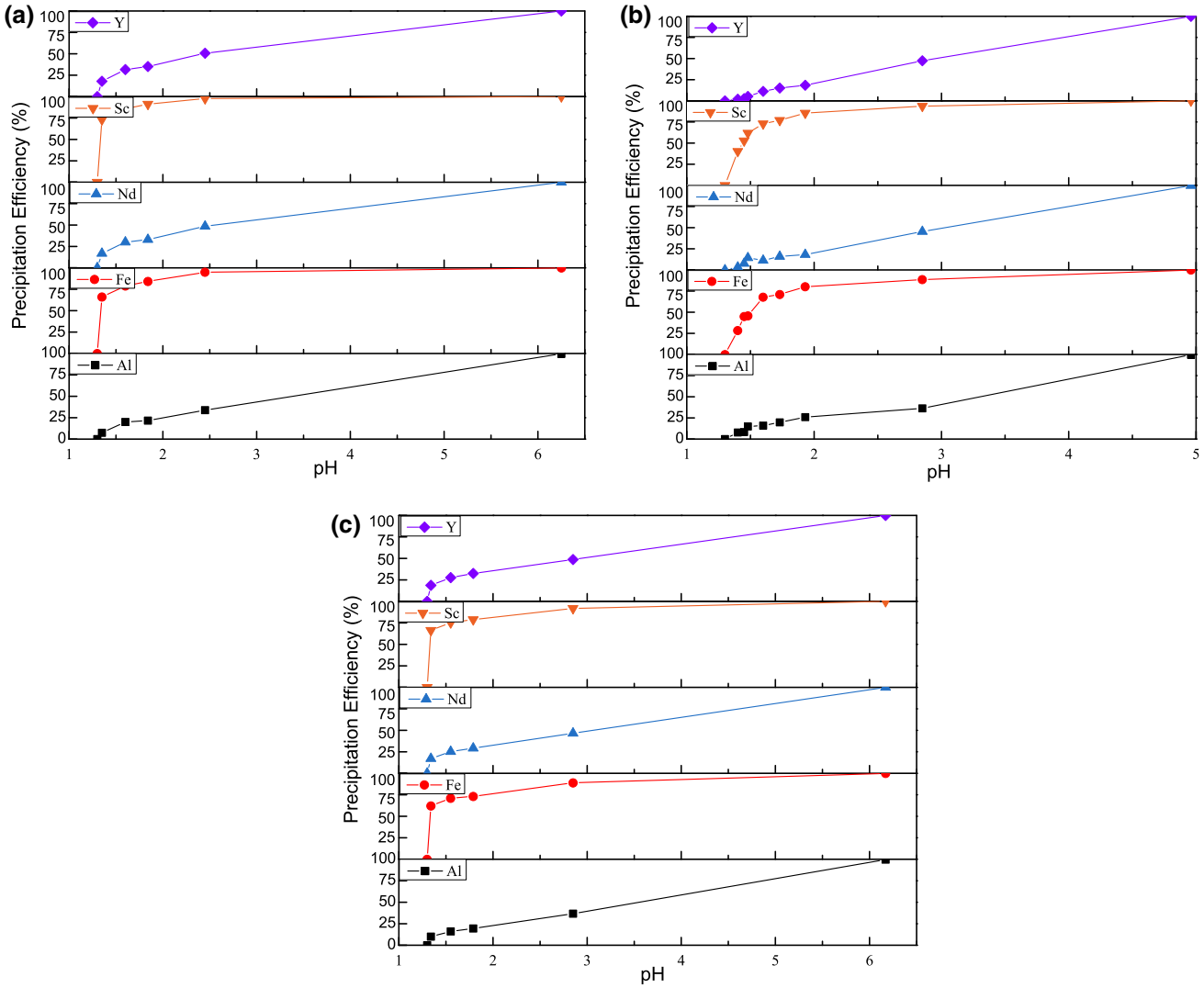

Fig. 5 Phosphate precipitation of synthetic red mud leachate solution by **a** K_2HPO_4, **b** $(NH_4)_2HPO_4$, and **c** Na_2HPO_4

Table 5 Critical pH values for above 80 % Sc recovery from the solution system by dibasic phosphate precipitation and the precipitation efficiencies of the constituent ions

Precipitation agent	pH	Fe(III) (%)	Sc (%)	Al (%)	Y (%)	Nd (%)
K_2HPO_4	1.84	84.2	91.2	21.6	35.1	33.1
K_2HPO_4	2.45	94.8	97.1	33.9	50.7	47.7
$(NH_4)_2HPO_4$	1.93	80.1	86.3	25.4	18.1	18.4
$(NH_4)_2HPO_4$	2.85	89.1	97.6	36.5	47.8	45.6
Na_2HPO_4	1.79	73.6	78.7	19.5	32.4	29.2
Na_2HPO_4	2.80	91.8	94.2	37.8	51.2	49.2

Table 6 Selectivity coefficients of Sc over Al, Y, and Nd for partial and almost complete Sc recovery from the solution by dibasic phosphate precipitation

Precipitation agent	pH	$S_{Sc/Al}$	$S_{Sc/Y}$	$S_{Sc/Nd}$
K_2HPO_4	1.84	38	19	21
K_2HPO_4	2.45	65	33	37
$(NH_4)_2HPO_4$	1.93	19	29	28
$(NH_4)_2HPO_4$	2.85	71	44	49
Na_2HPO_4	1.79	15	8	9
Na_2HPO_4	2.80	27	15	17

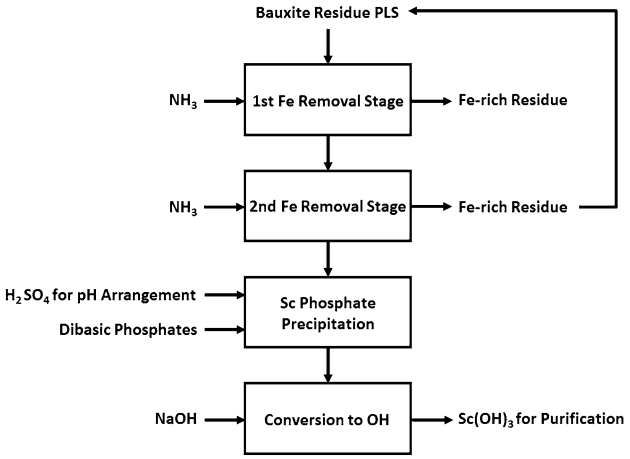

Fig. 6 Proposal flow sheet for Sc recovery from bauxite residue PLS

Assessment and Conclusion

Two different precipitation approaches were tested on synthetic red mud pregnant leach solution for recovery of Sc from sulfate media. Different hydroxide donors such as limestone, NaOH, NH_3(aq), and KOH were investigated, and among those, NH_3(aq) showed superior performance in the removal of Fe(III) from the system and had the lowest co-precipitation percentages of the remaining species in solution. While above 90 % of the Fe(III) was removed from the solution, Sc losses owing to co-precipitation with Fe(III) were 4 % at pH 3.5. At pH 3.35, almost 75 % Fe can be removed, while Sc losses were approximately 1.5 %. A two-step process for Fe removal is proposed prior to final Sc separation from the PLS.

The other approach examined is phosphate precipitation using dibasic phosphate solutions as the precipitant. As a consequence of addition of dibasic phosphate to the synthetic PLS, almost instantaneous and selective Sc and Fe precipitation was achieved. $(NH_4)_2HPO_4$ exhibited greater yield in terms of Sc and Fe(III) precipitation with minimal Al and REEs co-precipitation. Selective Sc separation is possible with dibasic phosphates only if Fe in the solution is removed beforehand.

Calcium, one of the major impurities in the BR, does not react with any of the precipitation agents introduced to the system; therefore, no additional steps are needed for Ca removal from the system. On the contrary to the problematic behavior of Fe(III) during various purification steps, co-precipitation with Sc, or loading, scrubbing, and stripping problems throughout solvent extraction, etc., aluminum remaining in the system can be removed with additional minor steps.

Taking into consideration the results attained from this study, a possible process route is proposed, which may be directly applicable to the highly impure PLS (Fig. 6). A dual-stage Fe removal process with ammonia solution addition prior to the final Sc recovery stage, by the addition of dibasic phosphate in the absence of Fe, in the PLS is proposed. This is expected to result in high yield and selectivity for the recovery of Sc from solution. To allow minimal losses of Sc during the second iron removal stage, the residue obtained from the second stage is recycled and used as seed material for the first stage of iron removal. Since this residue contains lower amount of Fe in its composition compared to the residue obtained by first Fe removal stage, recycling it directly into the PLS will not affect the initial composition drastically and will provide a driving force for nucleation/precipitation. The resulting $ScPO_4$ precipitate produced, which contains a small amount of Al and REEs, can be converted into hydroxide, via dissolution in NaOH for further product purification.

To enhance the efficiency of the process, kinetics and the temperature dependence of the mentioned reactions have to investigated in more detail.

Acknowledgments The research leading to these results has received funding from the European Community's Horizon 2020 Programme ([H2020/2014–2019]) under Grant Agreement No. 636876 (MSCA-ETN REDMUD). This publication reflects only the author's view, exempting the Community from any liability. Project website: http://www.etn.redmud.org.

References

1. Lathabai S, Lloyd P (2002) The effect of scandium on the microstructure, mechanical properties and weldability of a cast Al–Mg alloy. Acta Mater 50(17):4275–4292
2. Lee S, Utsunomiya A, Akamatsu H, Neishi K, Furukawa M, Horita Z, Langdon T (2002) Influence of scandium and zirconium on grain stability and superplastic ductilities in ultrafine-grained Al–Mg alloys. Acta Mater 50(3):553–564
3. Marquis E, Seidman D (2001) Nanoscale structural evolution of Al_3Sc precipitates in Al(Sc) alloys. Acta Mater 49(11):1909–1919
4. Ormerod RM (2003) Solid oxide fuel cells. Chem Soc Rev 32(1):17–28

5. Yamamoto O (2000) Solid oxide fuel cells: fundamental aspects and prospects. Electrochim Acta 45(15):2423–2435
6. Feuling RJ (1991) Recovery of scandium, yttrium and lanthanides from titanium ore. US Patent 5,049,363
7. Gongyi G, Yuli C, Yu L (1988) Solvent extraction off scandium from wolframite residue. JOM 40(7):28–31
8. Wang W, Cheng CY (2011) Separation and purification of scandium by solvent extraction and related technologies: a review. J Chem Technol Biotechnol 86(10):1237–1246
9. Wang W, Pranolo Y, Cheng CY (2011) Metallurgical processes for scandium recovery from various resources: a review. Hydrometallurgy 108(1):100–108
10. Power G, Gräfe M, Klauber C (2011) Bauxite residue issues: I. Current management, disposal and storage practices. Hydrometallurgy 108(1):33–45
11. Borra CR, Pontikes Y, Binnemans K, Van Gerven T (2015) Leaching of rare earths from bauxite residue (red mud). Miner Eng 76:20–27
12. Ochsenkühn-Petropoulou MT, Hatzilyberis KS, Mendrinos LN, Salmas CE (2002) Pilot-plant investigation of the leaching process for the recovery of scandium from red mud. Ind Eng Chem Res 41(23):5794–5801
13. Ochsenkühn-Petropulu M, Lyberopulu T, Ochsenkühn K, Parissakis G (1996) Recovery of lanthanides and yttrium from red mud by selective leaching. Anal Chim Acta 319(1):249–254
14. Wang W, Pranolo Y, Cheng CY (2013) Recovery of scandium from synthetic red mud leach solutions by solvent extraction with D2EHPA. Sep Purif Technol 108:96–102
15. Ochsenkühn-Petropulu M, Lyberopulu T, Parissakis G (1995) Selective separation and determination of scandium from yttrium and lanthanides in red mud by a combined ion exchange/solvent extraction method. Anal Chim Acta 315(1):231–237
16. Horovitz CT (2012) Scandium its occurrence, chemistry physics, metallurgy, biology and technology. Academic Press, London
17. Chen PL, Chen IW (1993) Reactive cerium (IV) oxide powders by the homogeneous precipitation method. J Am Ceram Soc 76(6):1577–1583
18. Li JG, Ikegami T, Mori T, Yajima Y (2004) Sc_2O_3 nanopowders via hydroxyl precipitation: effects of sulfate ions on powder properties. J Am Ceram Soc 87(6):1008–1013
19. Stevenson PC, Nervik WE (1961) The radiochemistry of the rare earths: scandium, yttrium, and actinium, vol 3020. National Academies, Washington, DC
20. Vickery RC (1960) The chemistry of yttrium and scandium, vol 2. Pergamon Press, Oxford
21. Firsching FH, Brune SN (1991) Solubility products of the trivalent rare-earth phosphates. J Chem Eng Data 36(1):93–95
22. Liu X, Byrne RH (1997) Rare earth and yttrium phosphate solubilities in aqueous solution. Geochim Cosmochim Acta 61(8):1625–1633
23. Lucas S, Champion E, Bregiroux D, Bernache-Assollant D, Audubert F (2004) Rare earth phosphate powders $RePO_4{\cdot}nH_2O$ (Re = La, Ce or Y)—part I. Synthesis and characterization. J Solid State Chem 177(4):1302–1311
24. Beltrami D, Deblonde GJ-P, Bélair S, Weigel V (2015) Recovery of yttrium and lanthanides from sulfate solutions with high concentration of iron and low rare earth content. Hydrometallurgy 157:356–362